RSC Advances

PAPER

View Article Online
View Journal | View Issue

Cite this: *RSC Adv.*, 2025, **15**, 11115

Water-soluble ZnPc(COOH)$_4$/Ch/MgO self-assembled systems

Tamara Potlog, *[a] Ion Lungu, [a] Mariana Diru,[a] Alexandrina Druta [b] and Marius Dobromir[c]

Received 20th February 2025
Accepted 20th March 2025

DOI: 10.1039/d5ra01256b

rsc.li/rsc-advances

In this study, a new metal oxide NP/MPc derivative composite as efficient photosensitizer for photodynamic therapy of cancer and photocatalytic activities is developed. The ZnPc(COOH)$_4$/MgO composite consists of the synthesized water soluble tetra-carboxy zinc phthalocyanine derivative and magnesium oxide nanoparticles prepared with different precipitating agents. The ZnPc(COOH)$_4$/MgO composites were investigated by UV-Vis spectroscopy and fluorescence spectrophotometry. The absorption and emission spectra of the self-assembled ZnPc(COOH)$_4$/MgO composite highlight the Stokes shift between them, which is near 119 nm. The composites also exhibited room-temperature phosphorescence with an average triplet state lifetime of 5.01 μs and a quantum yield of 10.63%.

Introduction

The exceptional properties of metal phthalocyanines (MPc) make them attractive in diverse fields ranging from technological, industrial, to medical.[1] Metal phthalocyanine, as an organic electron donor with high melting and boiling points, stable structure, and high light utilization rate, can produce O_2^- and OH^- radicals, as well as singlet oxygen $^1O_2$ that can degrade pollutants under light. The ability to fluoresce and simultaneously generate active oxygen metabolites allows the use of these compounds in theranostics.[2–5] Metal phthalocyanines derivatives can be also considered as promising photosensitizers for photodynamic therapy (PDT) of cancer.[6–9] The main problem of all "flat" tetrapyrrole macrocycles is their tendency to aggregate.[10] This problem is solved by introducing various peripheral functional groups that prevent active π–π-stacking of the macrorings, as well as by using a complexing metal that can be located above the plane of the macroring. Anionic water-soluble phthalocyanines are obtained by introducing sulfo and carboxy groups, linked to the ring directly or through linkers. Zinc phthalocyanine derivatives containing electron-donating thiol groups,[11–13] electron-withdrawing carboxyl groups[14–16] or electron-accepting sulfonyl groups[17,18] have been synthesized to improve water solubility. The preparation of sulfonated phthalocyanines and their complexes can be carried out by the template assembly method from a sulfonated precursor or by sulfonation of the phthalocyanine itself.[19] The disadvantage of the latter method is low regioselectivity.[20] The synthesis of metal phthalocyanine complexes containing a carboxyl group is highly resistant to oxidation and photo destruction.[21–25] Due to this, they are considered as promising materials for photodynamic therapy of oncological diseases. Presently, modern trends in the use of conjugates of nanoparticles with macrocyclic compounds are actively developing and show that the direction of further research will be focused on the implementation of the idea of developing the next generation of theranostic agents based on metal phthalocyanine derivatives and metal nanoparticles (Au, Ag NPs)[26,27] Nanoparticles can be used simultaneously as an antenna, a diagnostic marker, and a platform for targeted delivery. The concept of developing a theranostic platform based on multifunctional phthalocyanine nanostructures has great potential for expanding the capabilities of modern medicine and the transition to modern personalized nanomedicine.[28,29] In general, MgO nanoparticles (NPs) have been synthesized using a variety of physical, chemical, and green approaches.[30–35] Highly luminescent magnesium oxide nanoparticles were synthesized by the sol–gel method.[36] Here, we propose MgO NPs synthesized by the co-precipitation method using sodium dodecyl sulfate (SDS), a well-known surfactant that improves the surface properties of nanoparticles, and aloe vera extract (AVE), which acts as an eco-friendly reducing agent and a non-hazardous gelling agent for stabilizing the nanostructures.

In this paper, tetra carboxy ZnPc derivative and MgO NPs are conjugated to form a new ZnPc(COOH)$_4$/MgO nanocomposite. We study the photophysical behavior of the composite which is essential for photosensitizers aimed for use in PDT.

[a]*Laboratory of Organic/Inorganic Materials for Optoelectronics, Institute of Applied Physics, Moldova State University, Chisinau, Republic of Moldova. E-mail: tpotlog@gmail.com*

[b]*Doctoral School "Natural Sciences", Moldova State University, Chisinau, Republic of Moldova*

[c]*Alexandru Ioan Cuza University of Iasi, Research Centre on Advanced Materials andTechnologies, Department of Exact and Natural Sciences, Institute of Interdisciplinary Research, 11 Carol I Blvd., 700506, Iasi, Romania*

Experimental part

Synthesis of MgO nanoparticles and ZnPc(COOH)$_4$/Ch/MgO self-assembled systems

MgO nanoparticles (NPs) were synthesized by the co-precipitation method using sodium dodecyl sulfate (SDS), a well-known surfactant that improves the surface properties of nanoparticles, and aloe vera extract (AVE), which acts as an eco-friendly reducing agent and a non-hazardous gelling agent for stabilizing the nanostructures.

According to the following procedure, 100 mL of magnesium nitrate solution was prepared by dissolving 5 g of $Mg(NO_3)_2 \cdot 6H_2O$ in deionized water. Separately, 0.288 g of sodium dodecyl sulfate and 0.8 g of NaOH were each dissolved in deionized water. The sodium dodecyl sulfate solution was gradually added in small portions to the magnesium nitrate solution under continuous stirring. Subsequently, the NaOH solution, which facilitates the precipitation reaction, was added dropwise every 3 minutes with constant stirring at a temperature of 70–80 °C for 2 hours. The formation of a white precipitate was observed. Sodium dodecyl sulfate hydrolyzes in aqueous solutions, creating a basic medium:

$$NaC_{12}H_{25}SO_4 \rightarrow Na^+ + C_{12}H_{25}SO_4^- \quad (1)$$

$$NaC_{12}H_{25}SO_4^- \rightarrow Na^+ + C_{12}H_{25}SO_4^- \quad (2)$$

Magnesium nitrate, a strong electrolyte, dissociates to form magnesium cations and nitrate anions. In a basic medium, magnesium cations precipitate as magnesium hydroxide, resulting in the formation of a white precipitate.

$$Mg^{2+} + 2OH \leftrightarrow Mg(OH)_2\downarrow \quad (3)$$

The precipitate was filtered through a blue-banded filter paper and washed with 50 mL of distilled water. The precipitate was dried at room temperature, with a synthesis yield of 65%. The residue was calcined at temperatures of 300 °C, 500 °C, and 700 °C. As a result of calcination at temperatures of 300 °C and 500 °C, the residues were brown and black, respectively. It can be concluded that magnesium oxide, which is white in color, was not formed at these temperatures. Calcination at 700 °C led to the formation of a white residue. At this temperature, magnesium hydroxide decomposes according to the reaction equation:

$$Mg(OH)_2 \rightarrow MgO + H_2O \quad (4)$$

A yielding of 1.161 g of the MgO nanoparticles were obtained *via* a controlled calcination process.

Chitosan has proven to be a highly versatile and effective multifunctional agent in the production and application of metal nanoparticles.[37] Therefore, one thousand milligrams of chitosan were dissolved in 100 mL of aqueous solution at 1% acetic acid. The mixture was continuously agitated for 20 hours at 60 °C to obtain the chitosan solution. Later, the prepared chitosan solution was mixed drop by drop with the MgO NPs. The synthesis of chitosan-functionalized MgO is indicated by the color change in the homogeneous solution after 5 hours of continuous stirring. The mixture was then transferred to a hot plate, dried at 100 °C, and calcined for 5 hours at 700 °C in a muffle furnace to produce chitosan-functionalized magnesium oxide nanoparticles. Structure of a chitosan-MgO nanocomposite is shown in Fig. 1a.

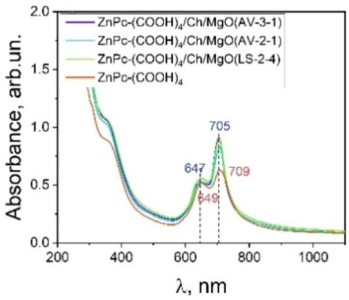

Fig. 1 UV-Vis spectra of ZnPc(COOH)$_4$ and ZnPc(COOH)$_4$/Ch/MgO in water.

Also, it is well known,[38,39] that substituted MPcs exhibit promising photosensitizing properties for photodynamic therapy (PDT) of cancer, demonstrating higher photodynamic properties. Solubility is a major challenge for MPcs. The solubility of unsubstituted MPcs is extremely low. Aqueous solutions suitable for spectroscopic and photochemical studies, with concentrations of about 10^{-6} mol L^{-1}, can only be obtained in DMSO or DMF. The developed tetra carboxy ZnPc derivatives (ZnPc(COOH)$_4$), displayed reasonable photo physicochemical behavior and photodynamic activity in DMSO/H_2O.[40] The conjugation of ZnPc(COOH)$_4$ to MgO NPs has not been reported in the literature. The current paper employed a method where chitosan was linked to MgO NPs before conjugating to ZnPc(COOH)$_4$.

Finally, 3 mg of (ZnPc(COOH)$_4$), solubilized in 3 mL of deionized water, was added to 0.2 mL of chitosan-surface-modified MgO nanoparticle solution and stirred for 2 hours in the dark. The product was centrifuged at 4500 rpm for 30 minutes, forming the MgO/Ch/ZnPc(COOH)$_4$ assembled system, as illustrated in Fig. 1b and Scheme 1.

Fortunately, peripheral carboxy (–COO^-) substituted ZnPcs can be easily prepared to dissolve in aqueous media and form homogeneous solutions.

Characterization technique

The structure of the ZnPc(COOH)$_4$/Ch/MgO composite was investigated by X-ray diffraction (XRD) using a Bruker-AXS D8 Advance diffractometer (CuKα radiation, 40 mA, 40 kV). The morphology and composition were examined using a TESCAN Vega TS 5130 MM (Brno, Czech Republic) scanning electron microscope (SEM) and energy dispersive X-ray spectroscopy (EDS) (Oxford, UK).

A Bruker Alpha FTIR spectrometer with a Diamond Crystal ATR accessory was used for rapid compound identification. The chemical composition of the ZnPc(COOH)$_4$/Ch/MgO compounds was further analyzed using an FT-IR 4600 spectrometer (Spectrum Research Systems Co.) in the mid-infrared

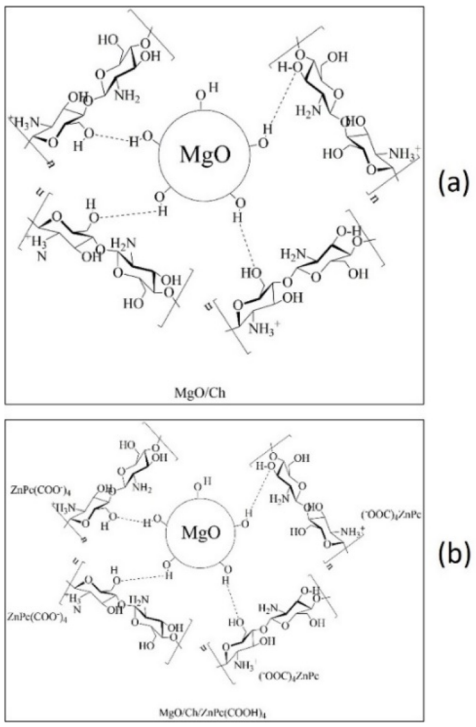

Scheme 1 Structure of MgO/Ch NPs (a) and MgO/Ch/ZnPc(COOH)$_4$ self-assembled system (b).

region, ranging from 4000 to 400 cm^{-1}. X-ray photoelectron spectroscopy (XPS) measurements were performed using a Physical Electronics PHI 5000 Versa Probe instrument, equipped with a mono-chromated AlK$_\alpha$ X-ray source ($h\nu$ = 1486.7 eV).

Results and discussion

Absorption and emission of MgO/Ch/ZnPc(COOH)$_4$ self-assembled systems

The UV-Vis absorption spectrum of ZnPc(COOH)$_4$ in water (Fig. 1) exhibits an intense "shoulder" peak (extinction coefficient >200 000) at approximately 380 nm (the Soret band), followed by a Q-band extending from 600 nm to 760 nm, with two maxima of subbands located around 647–649 nm and 705–709 nm, respectively.

To enhance the efficacy of photodynamic therapy, we conjugated ZnPc(COOH)$_4$ to MgO/chitosan nanoparticles through the free –OH and –NH$_2$ groups of chitosan.

According to Fig. 1, the conjugation of ZnPc(COOH)$_4$ to MgO/chitosan nanoparticles does not result in change in the position of the bands observed in tetracarboxy ZnPc, except for a modification in the intensity of both bands. The "shoulder" peak is likely an unresolved vibrational-electronic (additional) transition. The splitting of the Q-band results from the overlap of the electronic transitions corresponding to the first two excited states and their associated vibrational levels. The typical assignment for the spectral bands in ZnPc is that the lower-energy peak corresponds to the S_1 state (n $\rightarrow$ π^*) and the higher-energy peak to the S_2 state ($\pi \rightarrow \pi^*$).

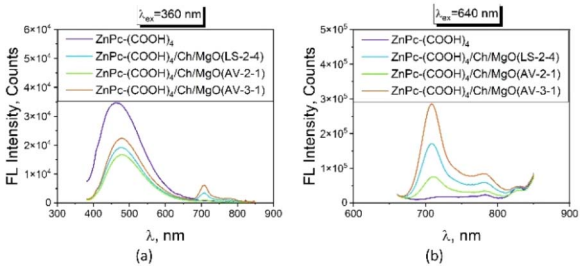

Fig. 2 Fluorescence spectra of ZnPc(COOH)$_4$ and ZnPc(COOH)$_4$/Ch/MgO systems excited with λ = 360 nm (a) and λ = 640 nm (b) in water.

The ZnPc(COOH)$_4$/Ch/MgO solutions, when excited at 360 nm (Fig. 2a), emit electromagnetic radiation (light) as a result of the transition from a higher to a lower electronic energy level.

The substitution of ZnPc with COOH groups causes a shift in the emission wavelength compared to pure ZnPc. The emission spectrum of ZnPc(COOH)$_4$ in water shows a broad, high-intensity emission band at 465 nm. According to the Franck-Condon principle, if a particular transition probability between the fundamental and 1st vibrational levels is the highest in absorption, the reverse transition is also most probable in emission.[41]

The emission and absorption transitions appear as mirror images if they correspond to electronic transitions between the same two states and if no significant molecular configuration changes occur in the excited state. The generally symmetric nature of these spectra results from the involvement of the same transitions in both absorption and emission and the similar vibrational energy levels of the S_0 and S_1 states.

For the ZnPc(COOH)$_4$/Ch/MgO self-assembled system, the primary emission band shifts to 479 nm, and an additional, weaker band appears at 707 nm. The fluorescence spectrum occurs at longer wavelengths than the absorption, a shift caused by energy losses due to the vibrational relaxation in the excited state. The difference between the absorption and the fluorescence maxima, known as the Stokes shift, is 105 nm for ZnPc(COOH)$_4$ and 119 nm for the ZnPc(COOH)$_4$/Ch/MgO system.

For the conjugated system excited at 640 nm, presented in Fig. 2b, additional lower-intensity bands also appear at 708 nm

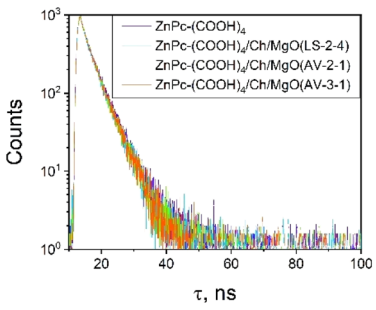

Fig. 3 Fluorescence lifetime spectra of the ZnPc(COOH)$_4$ and ZnPc(COOH)$_4$/Ch/MgO self-assembled systems in water.

Table 1 Fluorescence lifetimes (τ_1 and τ_2), average lifetime, relative contribution (%Rel), and quantum yield of fluorescence

	Fluorescence					
Samples	τ_1, ns	τ_2, ns	τ_{av}, ns	Rel_{τ_1}, %	Rel_{τ_2}, %	Φ, %
$ZnPc(COOH)_4$	1.50	4.44	2.97	25.22	74.78	21.17
$ZnPc(COOH)_4$/Ch/MgO (LS-2-4)	1.31	4.21	2.76	24.08	75.92	4.21
$ZnPc(COOH)_4$/Ch/MgO (AV-2-1)	1.59	4.21	2.90	25.85	74.15	4.24
$ZnPc(COOH)_4$/Ch/MgO (AV-3-1)	1.31	4.06	2.66	18.11	81.89	3.99

and 782 nm. When excited at 640 nm, only the $ZnPc(COOH)_4$/Ch/MgO systems exhibit the same emission bands at 708 nm and 782 nm, as observed with 360 nm excitation. The fluorescence intensity of $ZnPc(COOH)_4$/Ch/MgO increases significantly due to the intramolecular proton transfer between the $ZnPc(COO^-)_4$ and the NH_3^+ groups of the MgO/chitosan nanoparticles.

Another notable feature in all prepared solutions is the emission band at 828 nm, likely resulting from excited-state reactions, complex formation, and/or charge-transfer complexes involving amines.

The fluorescence lifetime of the $ZnPc(COOH)_4$ and $ZnPc(COOH)_4$/Ch/MgO systems is presented in Fig. 3. The excitation wavelength was $\lambda_{ex} = 365$ nm, and the emission wavelength was set at 338 nm. $ZnPc(COOH)_4$ in an H_2O solution displays a bi-exponential decay, clearly indicating the presence of two distinct species populations. Lifetimes were estimated to use the least squares fitting technique with a bi-exponential decay model. The fluorescence decay for each sample was fitted to the following bi-exponential function:

$$I(t) = a_1 \exp\left(-\frac{t}{\tau_1}\right) + a_2 \exp\left(-\frac{t}{\tau_2}\right) \quad (5)$$

where τ_1 and τ_2 are the lifetimes of the two decay components, and a_1 and a_2 are their respective amplitudes. Here, t represents the time from excitation, and τ is the time required for the intensity to decrease to $1/e$ (≈ 0.368) of its initial value.

The quality of the fit was evaluated using the reduced chi-square (χ^2) test and deviation function criteria. After fitting the intensity decay curves, the extracted lifetime values are presented in Table 1.

As summarized in Table 1, both the $ZnPc(COOH)_4$ and $ZnPc(COOH)_4$/Ch/MgO systems in water exhibit two characteristic fluorescence lifetimes with an average lifetime of approximately 3 ns, slightly higher for the self-assembled system. The concentration of $ZnPc(COOH)_4$ in water and in all $ZnPc(COOH)_4$/MgO/Ch/systems is 2 mg mL^{-1}. The absolute quantum yield of fluorescence of $ZnPc(COOH)_4$ reaches 21.17%, while for $ZnPc(COOH)_4$/Ch/MgO systems, it decreases to approximately 4%.

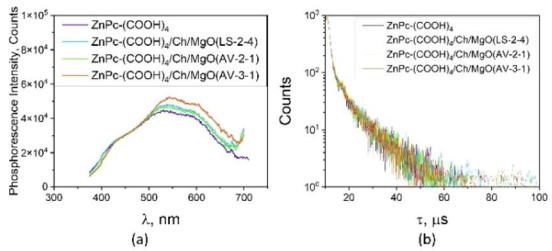

Fig. 4 Phosphorescence spectra of the $ZnPc(COOH)_4$ and $ZnPc(COOH)_4$/Ch/MgO self-assembled systems in water and the triplet excited state lifetimes of these systems.

Phosphorescence of MgO/Ch/$ZnPc(COOH)_4$ self-assembled systems

According to Fig. 4, both the $ZnPc(COOH)_4$ and $ZnPc(COOH)_4$/MgO/chitosan systems exhibit phosphorescence at room temperature.

The triplet excited state lifetime of the $ZnPc(COOH)_4$ and $ZnPc(COOH)_4$/MgO/Ch systems, under 355 nm excitation, displays a bi-exponential decay. The corresponding lifetime values are presented in Table 2. For the $ZnPc(COOH)_4$/MgO/Ch system, the highest lifetime value of approximately 5 μs was recorded. The phosphorescence quantum yield of this system reaches 10.63%.

To summarize, the present study facilitates the development of new sustainable room-temperature phosphorescent materials. This result indicates that the interaction between $ZnPc(COOH)_4$ and MgO/Ch was strong, which was beneficial for restricting the molecular vibrations of MgO/Ch and promoting

Table 2 Phosphorescence lifetimes (τ_1 and τ_2), average lifetime, relative contribution (%Rel), and quantum yield of phosphorescence

	Phosphorescence					
Samples	τ_1, μs	τ_2, μs	τ_{av}, μs	Rel_{τ_1}, %	Rel_{τ_2}, %	Φ, %
$ZnPc(COOH)_4$	1.04	8.47	4.76	57.67	42.33	3.20
$ZnPc(COOH)_4$/Ch/MgO (LS-2-4)	1.16	8.89	5.03	63.01	36.99	10.63
$ZnPc(COOH)_4$/Ch/MgO (AV-2-1)	1.13	8.83	4.98	61.39	38.61	0.01
$ZnPc(COOH)_4$/Ch/MgO (AV-3-1)	1.06	8.53	4.76	59.65	40.35	2.27

room-temperature phosphorescence emission. Room-temperature phosphorescence offers several significant advantages for optical detection, including enhanced selectivity and sensitivity, longer emission lifetimes, and a greater spectral shift between excitation and emission spectra. The extended lifetime of the triplet excited state facilitates the development of relatively inexpensive detection systems based on decay time measurements.

Conclusions

Attempts to enhance the photophysical properties of self-assembled systems have largely focused on conjugation of ZnPc derivatives to MgO/Ch NPs. The self-assembly of $ZnPc(COOH)_4$ to MgO/Ch NPs were shown to affect the quantum yield of fluorescence of ZnPc derivative, while provides a useful reference for the rational design of room-temperature phosphorescent material. The $ZnPc(COOH)_4$/Ch/MgO self-assembled system shows relatively high efficiency and long lifetime. So, we succeeded in the development of room-temperature phosphorescent material, $ZnPc(COOH)_4$/Ch/MgO, soluble in water. The preparation procedure was very simple and led to an effective room-temperature phosphorescent emission with a lifetime of 5.01 μs and a phosphorescence quantum yield of 10.63%.

It is shown that the triplet energies can be determined based on the strong spin–orbit coupling of Zn^{2+} ions: the first triplet energy can be evaluated by observing spin-forbidden singlet–triplet (S_0–T_1) absorption, whereas the second triplet energy was determined by intersystem crossing.

Data availability

The data that support the findings of this study are available from the corresponding author upon reasonable request.

Author contributions

Mariana Diru carried out the synthesis of MgO nanoparticles and their coating with chitosan. Alexandrina Druta was in charge of assembling the MgO/Ch NPs with $ZnPc(COOH)_4$ derivatives. Ion Lungu and Marius Dobromir conducted the measurements, and Tamara Potlog interpreted the results and wrote the paper.

Conflicts of interest

There are no conflicts to declare.

Acknowledgements

This paper was financially supported by the Ministry of Education and Research of the Republic of Moldova, MSU, under the subprogram "Designing Supramolecular Architectures Based on Metal Phthalocyanine Derivatives and Functionalized Nanoparticles for Medical Applications," #011209.

References

1 O. Koifman, T. Ageeva, I. Beletskaya, A. Averin, A. Yakushev, L. Tomilova and T. Dubinina, *Makporetepounknbi*, 2020, **13**, 311.
2 A. Pashkovskaya, I. Perevoshchikova, V. Maizlish, G. Shaposhnikov and E. Kotova, *Biochemistry*, 2009, **74**, 1021.
3 P. Lo, M. Rodríguez-Morgade, R. Pandey, D. Ng, T. Torres and F. Dumoulin, *Chem. Soc. Rev.*, 2020, **49**, 1041.
4 C. Claessens, U. Hahn and T. Torres, *Chem. Rec.*, 2008, **8**, 75.
5 A. Günsel, A. Bilgiçli, C. Kandemir, R. Sancak and G. Arabaci, *Synth. Met.*, 2020, **260**, 116288.
6 N. Simelane, G. Matlou and H. Abrahamse, *J. Mol. Sci.*, 2023, **24**, 1902.
7 T. Stuchinskaya, M. Moreno, M. Cook, D. Edwards and D. Russell, *Photochem. Photobiol. Sci.*, 2011, **10**, 822.
8 H. Montaseri, N. Simelane and H. Abrahamse, *Front. Nanotechnol.*, 2022, **4**, 928010.
9 L. Alonso, R. Sampaio, T. Souza, R. Silva, N. Neto, A. Ribeiro and A. Alonso, *J. Photochem. Photobiol., B*, 2016, **161**, 100.
10 A. Martinez De Pinillos Bayona, P. Mroz, C. Thunshelle and M. Hamblin, *Chem. Biol. Drug Des.*, 2017, **89**, 192.
11 F. Sarı, M. Kazici, E. Harputlu, S. Bozar, Ö. Koyun, Y. Sahin, N. Ugur, M. Ince and S. Günes, *ChemistrySelect*, 2018, **3**, 13692.
12 K. Ozoemena and T. Nyokong, *Microchem. J.*, 2003, **75**, 241.
13 M. Ke, C. Wang, Q. He, R. Que, Y. Wei, B. Zheng, X. Li, S. Huang and J. Huang, *Dyes Pigm.*, 2024, **227**, 112169.
14 K. Sakamoto and E. Ohno-Okumura, *Materials*, 2009, **2**, 1127.
15 G. Tunç, B. Canımkurbey, B. Dedeoğlu and Y. Zorlu, *J. Mol. Struct.*, 2021, **1240**, 130545.
16 L. Sun, X. Jin, T. Su, A. Fisher and X. Wang, *Adv. Mater.*, 2024, **36**, 2306336.
17 S. Bednarik, J. Demuth, J. Kernal, M. Miletin, P. Zimcik and V. Novakova, *Inorg. Chem.*, 2024, **63**, 8799.
18 F. Sarı, M. Kazici, E. Harputlu, S. Bozar, Ö. Koyun, Y. Sahin, N. Ugur, M. Ince and S. Günes, *ChemistrySelect*, 2018, **3**, 13692.
19 K. Palewska, J. Sworakowski and J. Lipiński, *Opt. Mater.*, 2012, **34**, 1717.
20 J. Kvíčala, M. Beneš, O. Paleta and V. Král, *J. Fluorine Chem.*, 2010, **131**, 1327.
21 Y. Li, J. Wu, J.-Z. Gu, W.-A. Qiu and A.-S. Feng, *Chin. J. Struct. Chem.*, 2020, **39**(4), 727–736.
22 A. Kalkan and Z. Bayır, *Polyhedron*, 2006, **25**, 39–42.
23 G. Shaposhnikov, V. Maizlish and V. Kulinich, *Russ. J. Gen. Chem.*, 2005, **75**, 1480.
24 J. Namgoong, H. Kim, S. Kim, S. Yuk, J. Choi and J. Kim, *Dyes Pigm.*, 2021, **184**, 108737.
25 M. Yanagisawa, F. Korodi, J. Bergquist, A. Holmberg, A. Hagfeldt, B. Åkermark and L. Sun, *J. Porphyrins Phthalocyanines*, 2004, **8**, 1228.
26 J. Xie, S. Lee and X. Chen, *Adv. Drug Delivery Rev.*, 2010, **62**, 1064.
27 S. Majeed, K. Sekhosana and A. Tuhl, *Arabian J. Chem.*, 2020, **13**, 8848.

28 V. Deivayanai, P. Thamarai, S. Karishma, A. Saravanan, P. Yaashikaa and A. Vickram, *Cancer. Pathog. Ther.*, 2024, **2**, E01.
29 L. Nene and H. Abrahamse, *Acta Pharm. Sin. B*, 2024, **14**, 1077.
30 M. Rafique, I. Sadaf, M. Rafique and M. Tahir, *Artif. Cells, Nanomed., Biotechnol.*, 2017, **45**, 1272.
31 M. Bandeira, M. Giovanela, M. Roesch-Ely, D. Devine and J. da Silva Crespo, *Sustainable Chem. Pharm.*, 2020, **15**, 100223.
32 Y. Yildiz, T. Okyay, B. Sen, B. Gezer, S. Kuzu, A. Savk, E. Demir, Z. Dasdelen, H. Sert and F. Sen, *ChemistrySelect*, 2017, **2**, 697.
33 H. Göksu, B. Çelik, Y. Yıldız, F. Şen and B. Kılbaş, *ChemistrySelect*, 2016, **1**, 2366.
34 B. Sen, A. Şavk and F. Sen, *J. Colloid Interface Sci.*, 2018, **520**, 112.
35 B. Şen, A. Aygün, A. Şavk, S. Akocak and F. Şen, *Int. J. Hydrogen Energy*, 2018, **43**, 20183.
36 A. Kumar, S. Thota, S. Varma and J. Kumar, *J. Lumin.*, 2011, **131**, 640.
37 I. Amor, H. Hemmami, N. Grara, O. Aidat, A. Amor, S. Zeghoud and S. Bellucci, *Polymers*, 2024, **16**, 2662.
38 K. Santos, R. Barros, D. da Silva Lima, A. Nunes, M. Sato, R. Faccio and J. Oshiro-Junior, *Photodiagn. Photodyn. Ther.*, 2020, **32**, 102032.
39 J. Algorri, M. Ochoa, P. Roldan-Varona, L. Rodriguez-Cobo and J. Lopez-Higuera, *Cancers*, 2021, **13**, 4447.
40 T. Potlog, A. Popusoi, I. Lungu, S. Robu and I. Bulimestru, *RSC Adv.*, 2022, **12**, 31778.
41 J. Lakowicz, *Principles of Fluorescence Spectroscopy*, University of Maryland School of Medicine Baltimore, 2006, p. 132.